Scientia Iranica (2024) 31(13), 1063–1076

Sharif University of Technology
Scientia Iranica
Transactions B: Mechanical Engineering
https://scientiairanica.sharif.edu

Research Note

Mechanical behavior and sliding wear assessment of Al2024/TiC metal matrix composite using Taguchi and spotted hyena optimization

R. Suresh[a,*], A.G. Joshi[b,1], M. Manjaiah[c], S. Kumar[d], and K.N. Bharath[e]

a. *Department of Mechanical and Manufacturing Engineering, MS Ramaiah University of Applied Sciences, Bangalore-560058, India.*
b. *Department of Mechanical Engineering, Canara Engineering College, Bantwal-574219, India.*
c. *Department of Mechanical Engineering, National Institute of Technology, Warangal, 506004, India.*
d. *Department of Mechanical Engineering, Symbiosis Institute of Technology, Pune-412115, India.*
e. *Department of Mechanical Engineering, G.M. Institute of Technology, Davangere-577006, India.*
1. *Present address: Department of Mechanical Engineering, Madanapalle Institute of Technology and Science, Madanapalle-517325, India.*

Received 6 January 2021; received in revised form 25 January 2022; accepted 4 March 2024

KEYWORDS
Metal matrix composite;
Sliding wear;
Taguchi;
Spotted hyena optimization.

Abstract. The microstructure, mechanical and tribological properties of Titanium Carbide (TiC) particles reinforced Al2024 Metal Matrix Composites (Al MMCs) were investigated. Fractography analysis of tensile test specimen revealed that debonding was prominent in 3% TiC reinforced Al MMCs, while clevage pattern failure was pronounced in 6% and 9% TiC reinforced MMCs. Tribological property was studied as sliding wear behaviour of MMCs. Analysis of Variance (ANOVA) analysis was employed to understand the effect of parameters, interaction effects was studied through response surface plots. Further, regression model was developed to correlate process parameters and wear. The worn surface analysis shown the formation of ridges and parallel furrows on surface in sliding direction. Al/TiC composites exhibited better mechanical properties and wear resistance compared to Al2024 alloy. The optimization of wear for its minimum value was achieved through spotted hyena optimization algorithm. The wear loss at optimized parameter was validated through experimental value and compared with Taguchi's technique.

1. Introduction

Metal Matrix Composites (MMCs) possess better physical, synthetic, mechanical, and tribological properties compared to monolithic metals, which makes them most reasonable for vast automobile and industrial applications. They comprise of metallic material incorporated with reinforcements like oxides, carbides, nitrides, etc. Thus, their incorporation imparts desired mechanical properties like higher transverse quality and solidness, noteworthy shear and compressive qual-

*. *Corresponding author.*
E-mail address: sureshchiru09@gmail.com (R. Suresh)

To cite this article:
R. Suresh, A.G. Joshi, M. Manjaiah, S. Kumar, and K.N. Bharath "Mechanical behavior and sliding wear assessment of Al2024/TiC metal matrix composite using Taguchi and spotted hyena optimization", *Scientia Iranica* (2024), **31**(13), pp. 1063-1076
https://doi.org/10.24200/sci.2024.57484.5261

ities and higher temperature abilities. MMCs were developed earlier with the goal to enhance execution for cutting edge military frameworks [1–3]. MMCs were extremely regarded for their superior material characteristics such as high specific stiffness, impact resistance and fracture resistance [4,5]. Nanoparticles reinforcement has increased drastically in the past decade. The nano-silicon carbide (SiC) reinforcement impart greater hardness, higher wear and corrosion resistance [6]. While nano-Titanium Carbide (TiC) reinforcement results high specific strength, excellent resistance to corrosion and wear [7].

The wear resistance of material relies on sliding surface asperity interaction. Wear resistance of aluminium (Al) alloys is poor, due to plastic deformation of smooth asperities at elevated temperatures [8]. Al composites with brittle reinforcements interact with the counterface and impart enhanced service life [9-11]. Increased resistance results in low asperity deformation, leading to wear surface abrasion [12]. The wear resistance of composites is decreased as the asperities are removed under severe circumstances. Due to abrasion, the wear debris from the surface are removed under low load conditions [13].

The modelling of wear behaviour of MMCs is highly significant for better understanding and prediction. Earlier studies have reported on utilization of different statistical and modelling techniques to correlate wear parameters with responses. Tarasasanka et al. [14] evaluated dry sliding wear behaviour of AZ91E/nano-Al_2O_3 MMCs. Optimization of wear rate and friction force was carried out using Taguchi-Grey relation analysis. Natrayan and Senthil Kumar [15] captured experimental results according to Taguchi L16 orthogonal array to study the influence of wear parameters on wear rate and coefficient of friction. Analysis of Variance (ANOVA) and regression analysis were employed to model the tribological behaviour of $Al/Al_2O_3/SiC/Gr$ hybrid MMCs. Arunkumar et al. [16] attempted to correlate wear parameters namely. applied load and different types of reinforcements. Also, optimization of wear rate was done to yield minimum wear rate using Taguchi technique. Miloradović et al. [17] employed Taguchi method to obtain minimum specific wear rate of ZA27/SiC/Gr MMC within the confidence interval and predicted minimum value was validate through confirmation test. Velavan et al. [18] analysed and predicted the wear behaviour of boron carbide and mica reinforced Al MMCs using Box-Behnken experimental design. Subsequently wear optimization of MMC was attained using desirability approach.

The recent literatures have focused on various soft computing techniques like evolutionary algorithm and metaheuritics approaches for wear modelling and optimization. Gangwar and Pathak [19] shown that improved bat algorithm trained Artificial Neural Network (ANN) predicts the specific wear rate of marble dust reinforced MMCs with enhanced convergence speed. Gangwar et al. [20] presented Adaptive Neuro-Fuzzy Intereference System (ANFIS) model to correlate wear parameter with wear loss with accuracy of 97.99% compared with experimental results. Stalin et al. [21] illustrated that ANN-Teaching Learning Based Optimization (ANN-TLBO) algorithm can be precisely used to optimize wear rate compared to Taguchi-Grey analysis technique. Joshi et al. [4] have achieved minimum wear loss using Ant-Lion Optimizer (ALO) algorithm compared to Taguchi technique. Aydin [22] has employed Linear Regression (LR), Support Vector Regression (SVR), ANN and Extreme Learning Machine (ELM) techniques to establish the model for the prediction of sliding wear volume loss of Al/Al_2O_3.

The literature review indicates that, ANN has been widely employed for modelling and prediction of wear behaviour of MMCs. The optimization of wear resistance charateristics has been performed with the help of various statistical and soft computing optimization techniques such as ALO, ELM technique, ANN-TLBO, etc. The feasibility of metaheuristic approaches are promising and exhibited great potential for optimization of wear characteristics of MMCs. Spotted Hyena Optimization (SHO) algorithm has been recently developed by Dhiman and Kumar [23] and Panda et al. [24] demonstrated great adequancy for its application in mechanical and materials engineering. Further, limited work reported on the adequate and feasible implementation of bio-inspired metaheuristic approaches to achieve optimal conditions for minimum wear rate of composites. Thus, current work aims to implement SHO algorithm for wear rate optimization of Al/TiC MMCs. In the present work, Al2024 aluminum alloy used as a matrix material that has various aerospace applications such as aircraft fuselage, commercial and military aircraft body, wing tension members and critical aircraft structures. TiC was used as reinforcements due to its high specific stiffness, strength, wear resistance, fatigue resistance and good thermal characteristics.

2. Materials and experimentation

2.1. Specimen preparation

The material used for the research is composite of Al2024 alloy and TiC reinforcement at different weight percentages. The composite aluminum metal matrix was produced by stir-casting method. It was synthesized in electrical induction furnace at 760°C by ex-situ technique. In the graphite crucible in induction furnace, boron carbide with a purity of 99% and 250 mesh size was used as raw material. At first, Al2024 alloy was melted into the graphite crucible at a temperature of 650°C from small pieces of measured

Table 1. Chemical composition of Al2024 alloy.

Si	Fe	Cu	Mn	Mg	Cr	Zn	Ti	Others	Balance
0.50	0.50	4.2	0.65	1.5	0.10	0.25	0.15	0.05	Aluminum

Table 2. Parameters and their levels.

Sl. No.	Parameters	1	2	3
A	wt.% of TiC	3%	6%	9%
B	Sliding distance (m)	400	800	1200
C	Load on pin (N)	10	20	30
D	Sliding velocity (m/sec)	0.5	1.0	1.5

quantity. Subsequently, preheated TiC at 500°C was manually introduced to the molten metal with the assistance of spatula, i.e., 1-2 g/sec and with the aid of mechanical stirrer. In order to achieve homogenized mixture, it was stirred continuously at a rate of 250–350 rpm for 15 min. The composites were prepared by varying 3, 6, 9 weight percentage of TiC. Table 1 depicts the chemical composition of Al2024 alloy used in the study.

2.2. Mechanical tests

The tensile and compression tests were carried out on a universal testing machine as per ASTM E8 and E9 standards. The tensile test was carried at a speed of 0.5 mm/min on specimens having a 9 mm diameter at 62.5 mm gauge length. The compression test was carried out at 0.3 mm/min on cylindrical specimen having dimension of 13 mm diameter and 25 mm length resulting L/D ratio of 2. The micro-Vickers hardness test was conducted on samples as per ASTM E384. Each value of mechanical properties reported in the current work is an average of five readings recorded.

2.3. Dry sliding wear test

Al2024/TiC composite cylindrical samples were tested for dry sliding wear with diameter of 10 mm and length of 50 mm as per ASTM G-99 standard. The pin was made in contact with rotating disc of EN-8 steel with 62 HRc. The experiment trials were employed on pin-on-disc tribometer (Make-DUCOM, Model-TR 20LE-M5). The weight percentage of TiC in MMC, sliding distance (m), normal load (N) and sliding velocity (m/s) were selected as study parameters (Table 2). The wear of pin was determined through mass loss method. The mass of pin before and after the experiment was determined using digital mass balance system with an accuracy of 0.1 mg. The wear loss was computed and studied as a function of volume loss. At each instant of before and after the conduction of experiment, pin and disc were cleaned using acetone to ensure that traces of wear debris was eliminated. Each trial run was repeated two times to obtain minimum experimental error.

2.4. Plan of experiments

Taguchi's L27 orthogonal array was used to plan the experimental trial for wear test. The plan of experimentswith obtained results are shown in Table 3. The combination of study parameters for each trial run as per orthogonal array is depicted as each row of the table. In contrast, 1st to 4th column indicates the study parameter with their level variation for each trial. The last column shows the obtained wear volume loss for the corresponding combination of parameters. The wear loss was analyzed using '*smaller the better*'. ANOVA study was employed to examine the contribution and significance of each input parameter and their interactions.

2.5. Spotted Hyena Optimization (SHO)

The SHO algorithm was recently developed by Dhiman and Kumar [23]. It is a metaheuristic approach with simple algorithmic structure and implementation is also simple. It is inspired by the hunting conduct of spotted hyenas. Generally, 4 categories of hyenas found namely spotted, striped, brown and aardwolf hyenas. Spotted hyenas were seen as generally enormous among their species and are exceptionally capable as talented hunters. When prey is sighted, they utilize sound similar to human laugh to communicate and to alarm among themselves. As Ilany et al. [25] depicts, spotted hyenas live in a bunch of 100 confided in companions. While so as to extend their system, they typically partner with confided in associate hyenas. The hyenas have the aptitude to recognize prey location through vision, smell and perceptibility strategy. Initially, they search and trace the prey location. In the subsequent stage, identified prey is being chased by the cohesive cluster of hyenas. It is very helpful and efficient to ensure greatest fit. The elite hyena possess pre-knowledge of prey location and other will update themselves in their location. Later, the prey being encircled by a cluster of hyenas. Finally, a group of hyenas will attack with the elite followed by different individual hyenas in the bunch. The hunting conduct is modeled and demonstrated in the following steps and Figure 1 depicts the flowchart;

Step 1. Encircling of prey: Spotted hyenas with pre-knowledge on the location of prey existence encircle them. Dhiman and Kumar [23] illustrated the social hierarchy of them. The authors considered current solution as objective or target close to optimum since search space not known a priori. At the same time, other search agents (hyenas) update their location once the best search solution is determined. The step is mathematically modeled as Eqs. (1) and (2):

$$\overrightarrow{D_h} = \left| \overrightarrow{B} \times \overrightarrow{P_p}(x) - \overrightarrow{P}(x) \right|, \tag{1}$$

$$\overrightarrow{P}(x+1) = \overrightarrow{P}(x) - \overrightarrow{E} \times \overrightarrow{D_h}, \tag{2}$$

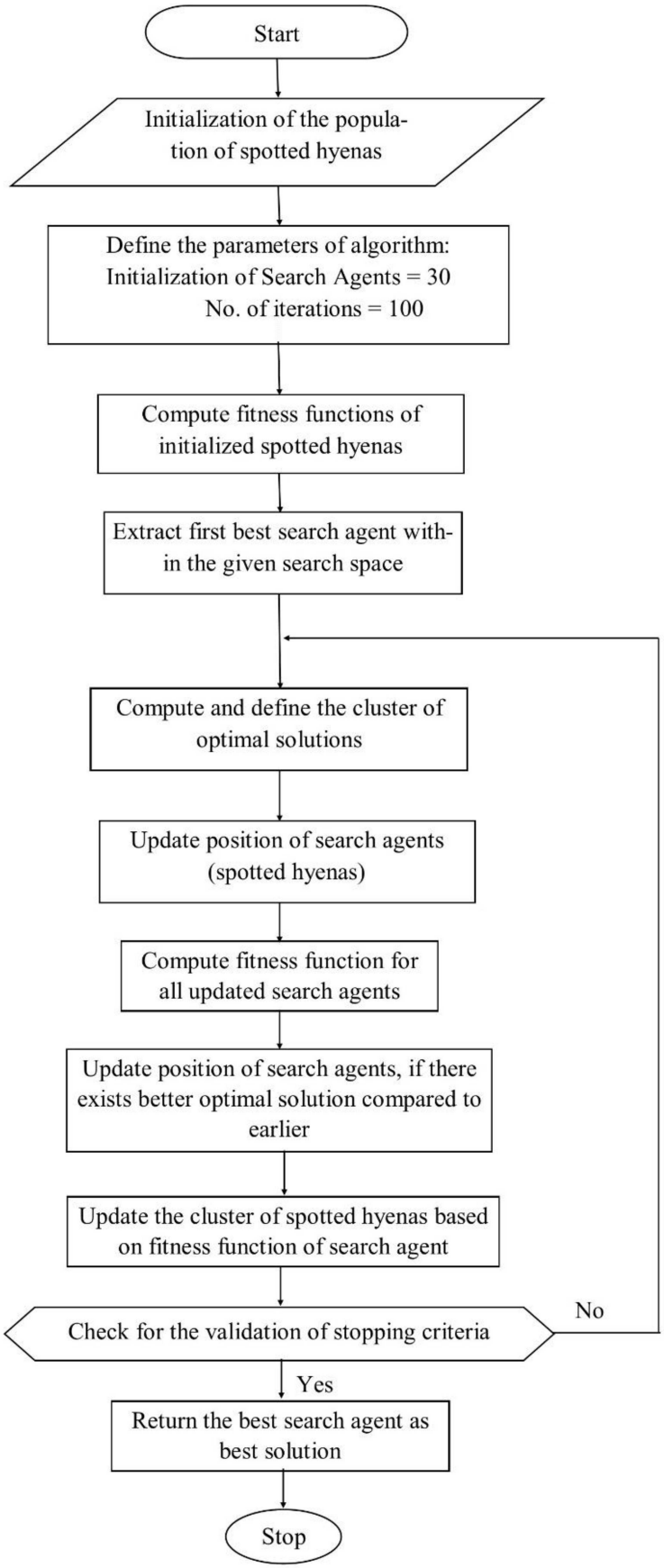

Figure 1. Flowchart of spotted hyena optimization.

Table 3. Experimental result as per L27 orthogonal with uncoded values of parameters.

Run No.	% of TiC (wt.%)	Sliding distance (m)	Average load (N)	Sliding velocity (m/s)	Wear loss (mm^3)
1	3	400	10	0.5	1.009
2	3	400	20	1.0	1.616
3	3	400	30	1.5	2.198
4	3	800	10	1.0	1.126
5	3	800	20	1.5	1.840
6	3	800	30	0.5	3.104
7	3	1200	10	1.5	0.989
8	3	1200	20	0.5	2.918
9	3	1200	30	1.0	2.524
10	6	400	10	0.5	0.761
11	6	400	20	1.0	1.158
12	6	400	30	1.5	1.532
13	6	800	10	1.0	0.621
14	6	800	20	1.5	1.262
15	6	800	30	0.5	2.361
16	6	1200	10	1.5	0.423
17	6	1200	20	0.5	1.891
18	6	1200	30	1.0	1.564
19	9	400	10	0.5	0.889
20	9	400	20	1.0	0.995
21	9	400	30	1.5	1.425
22	9	800	10	1.0	0.458
23	9	800	20	1.5	0.894
24	9	800	30	0.5	1.617
25	9	1200	10	1.5	0.241
26	9	1200	20	0.5	1.146
27	9	1200	30	1.0	0.872

where $\overrightarrow{D_h}$ denotes separation length of spotted hyena and prey, x means the present iteration, $\overrightarrow{B}$ and $\overrightarrow{E}$ are vectors of coefficient, $\overrightarrow{P_p}$ and $\overrightarrow{P}$ denotes the location vectors of prey and spotted hyenas, respectively. While absolute value and multiplication with vectors are denoted as $\|$ and $\times$, respectively. The $\overrightarrow{B}$ and $\overrightarrow{E}$ vectors are determined as follows:

$$\overrightarrow{B} = 2 \times r\overrightarrow{d_1}, \tag{3}$$

$$\overrightarrow{E} = 2\overrightarrow{h} \times r\overrightarrow{d_2} - \overrightarrow{h}, \tag{4}$$

$$\overrightarrow{h} = 5 - \left(iteration \times \frac{5}{\text{Max}_{\text{iteration}}}\right), \tag{5}$$

where $iteration = 1, 2, 3, \cdots, \text{Max}_{iteration}$. For the true reconciliation of exploitation and exploration, $\overrightarrow{h}$ directly reduces from 5 to 0 owing to the maximum iterations, $r\overrightarrow{d_1}$ and $r\overrightarrow{d_2}$ are random vectors lie in the interval of [0,1]. Further, $\overrightarrow{B}$ and $\overrightarrow{E}$ vectors are manipulated such that hyenas can reach different sites with respect to the current position. The present position of spotted hyenas updates their location randomly around the hunting prey using Eqs. (1) and (2). Thus, identical knowledge can be applied for n-dimensional search space exploration.

Step 2. Hunting: Generally, spotted hyenas lead life and catch prey in clusters. They rely on acquaintances and the capability to locate the victim. The mathematical representation of this conduct, the assumption was made that the best search agent possesses prior knowledge of the locality of prey. At the same time, other search agents form a group and assemble towards the best individual hyena. The mathematical representation of hunting prey behavior is illustrated as following Eqs. (6)-(8):

$$\overrightarrow{D_h} = \left|\overrightarrow{B} \times \overrightarrow{P_h} - \overrightarrow{P_k}\right|, \tag{6}$$

$$\overrightarrow{P_k} = \overrightarrow{P_h} - \overrightarrow{E} \times \overrightarrow{D_h}, \tag{7}$$

$$\overrightarrow{C_h} = \overrightarrow{P_k} + \overrightarrow{P_{k+1}} + \cdots + \overrightarrow{P_{k+N}}, \tag{8}$$

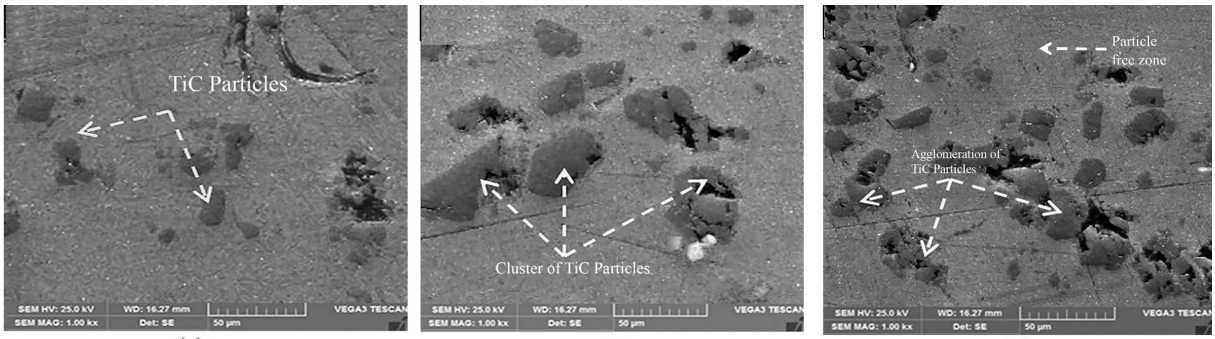

Figure 2. SEM images of (a) Al2024+3%TiC, (b) Al2024+6%TiC, and (c) Al2024+9%TiC metal matrix composites.

where $\overrightarrow{P_h}$ defines the location of first feasible solution (hyena) and $\overrightarrow{P_k}$ represents the location of other spotted hyenas. Furthermore, N denotes the number of hyenas that can be computing using Eq. (9):

$$N = count_{no.}\left(\overrightarrow{P_h}, \overrightarrow{P_{h+1}}, \overrightarrow{P_{h+2}}, ..., \left(\overrightarrow{P_h} + \overrightarrow{M}\right)\right), \quad (9)$$

where $\overrightarrow{M}$ is vector randomly lies in the interval of [0.5,1], *no.* suggests the number of solutions and count all candidate solutions and $\overrightarrow{C_h}$ indicates the set of N number of optimum solutions.

Step 3. Attacking prey: The mathematical model summarizing the attack on prey has been presented as Eq. (10). Simultaneously, $\overrightarrow{h}$ vector value is reduced. The reduction in the deviation in $\overrightarrow{E}$ vector is done to manipulate the value of $\overrightarrow{h}$ vector, which diminishes from 5 to 0 through iterations.

$$\overrightarrow{P}(x+1) = \frac{C_h}{N}, \quad (10)$$

where $\overrightarrow{P}(x+1)$ stores best fitness solution, while other spotted hyenas update their location based on the location of the best search agent (hyena). The algorithm permits its search agents to update their location and attacks on prey.

Step 4. Searching prey: The searching agents explore the prey based on the position of their location in crowd, which can be traced as vector $\overrightarrow{C_h}$. The vector $\overrightarrow{B}$ is deliberately required in this algorithm for the purpose of exploration and give randomly varied values during iteration. During, decline in the magnitude of vector $\overrightarrow{B}$, when $\overrightarrow{E} > 1$ about 50% of total iterations concentrate to explore while rest of the iterations exploit at $\overrightarrow{E} < 1$. Thus, $\overrightarrow{B}$ lies in the interval of 0 to 2 indicating random weights for prey. Subsequently, realizes the significance or insignificance of prey distance. This is helpful in attaining global optimum through the prevention of local optimum until the last iteration. Subsequently, the termination of optimization algorithm after meeting the goal of stopping criteria.

3. Results and discussions

3.1. Microstructural characterization of Al2024 alloy and its TiC MMCs

The microstructure of composites is carried out using Scanning Electron Microscope (SEM). Surfaces were machined and polished, followed by etching using Keller's reagent to obtain surface finish suitable for microstructure analysis. Samples were prepared (sample size ⌀ 12 mm × 12 mm length) as per the ASTM E3 standard. Figure 2(a), (b), and (c) shows SEM images of Al2024/TiC MMCs with variation of TiC reinforcement 3%, 6%, and 9% respectively. The microstructure reveals the nearly uniform distribution of TiC particles with negligible porosity in all the cast composite samples. Microstructure comprises of fine encourages in a framework of dendritic Aluminum strong arrangement. Agglomeration of reinforcement was also found minimum. Therefore, it can be inferred that, reinforcement particles dispersion in the matrix is nearly uniform.

3.2. Mechanical behavior

The resultant mechanical properties of fabricated MMCs are summarized in Table 4. It indicates that ultimate tensile strength, yield strength, compressive strength and hardness have increased with the increase of TiC percentage. While the percentage of elongation was found to decrease drastically. The obtained results ensure particulate strengthening mechanism owing to the arrest of dislocation movement present in the matrix. Further, an increase in TiC content results in the increase of strain energy required for the propagation of material imperfections. Thus, studied MMCs need greater amount of elastic energy for deformation. Therefore, increased values were recorded. Whereas ductility studied as a function of percentage of elongation has decreased with an increase in TiC content. It perhaps, TiC particles are ceramic and hard in nature. They can deform only through elastic energy and greater local matrix strain is necessary to occur deformation plastically. As a

Table 4. Mechanical properties of the different studied composite specimen.

Specimen	Mechanical properties				
	Ultimate tensile strength (MPa)	Yield strength (MPa)	% of elongation	Compressive strength (MPa)	Vickers hardness number (HV)
Al2024+3%TiC	201.5	106.4	11.6	229.1	86.4
Al2024+6%TiC	209.7	112.7	10.1	237.6	89.1
Al2024+9%TiC	217.2	124.9	8.4	241.9	93.8

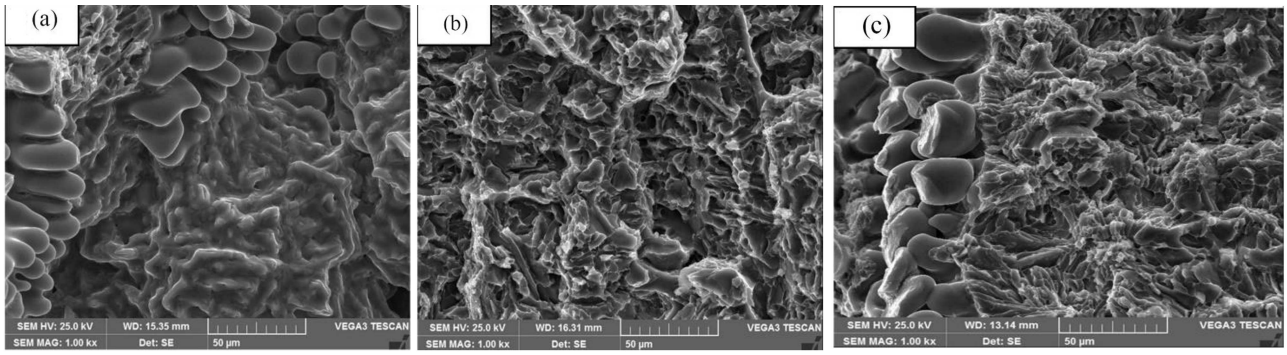

Figure 3. Fractographic images of (a) Al2024+3%TiC MMC, (b) Al2024+6%TiC MMC, and (c) Al2024+9%TiC MMCs.

result, matrix stresses get increases and local maximum stress also shoots up to higher value due to increased dislocation density and grain size [26]. Furthermore, the magnitude of required local strain increases with an increase in hard reinforcement particle number in a unit volume of MMCs. Hence, ductility diminishes with the reinforcement percentage increase. Therefore, the increase of TiC reinforcement within its studied range was found to be lucrative to impart greater mechanical properties to Al alloy at a reasonable cost of ductility.

3.3. Fractography studies of tensile test specimens

The fractographic SEM images (Figure 3) reveal the fracture surface after test. The dimples, dendrites and TiC particles are observed. The cleavage fracture pattern is observed in the 6% and 9% reinforcements. The 3% TiC reinforced Al composite fracture occurred along the grain boundaries, it is revealed by the dendrites, and de-bonding between the particle and matrix. The combined dendritic de-bonding and brittle fracture caused an increase in tensile strength and decrease of percentage elongation of the Al/TiC composites.

When the reinforcements square measure additional, the particulate cavalries type nuclei, which end in the bigger numeral of smidgen formation, therefore the movement is restricted additional, which ends in more significant strength. Consequently, the observation within the overall increase of the lastingness is with competence, even and interpretable. The SEM micrographs of the fracture surfaces of the tensile take a look at specimen square measure shows that the fracture may be expected from a ductile fracture in Al2024 alloy and brittle fracture in 2024/TiC composites.

3.4. Dry sliding wear behavior

The wear tests have been conducted for Al2024/TiC MMC as per L27 orthogonal array and obtained results are shown in Table 3. Experimental results are evaluated using MINITAB-17 Software package and are analyzed using *Smaller the better* criteria.

3.4.1. ANOVA and regression analysis

ANOVA was performed to determine the parameters that substantially affect wear rate. Table 5 demonstrates ANOVA and parameters affecting wear rate and their interactions. The p-value assessment was conducted for 95% confidence value and significance level of $\alpha = 0.05$. In Table 5, 7th column indicates the p-value of each parameter and for interaction of parameters. The last column indicates the percentage contribution of each parameter. It indicates that applied load, TiC%, sliding velocity and TiC% versus sliding distance interaction were found as significant with p-value <0.05. The percentage of contribution column indicates that the normal load is a highly significant parameter followed by % of TiC and sliding distance. Besides, sliding distance and interaction parameters were insignificant. Thus, individual parameter namely normal load, % of TiC and sliding velocity

Table 5. Analysis of variance for wear rate.

Parameters	Sum of squares	DOF	Variance	*F*-value	*F*-test	*p*-value	% of contribution
Normal load	6.5939	2	3.29695	104.27	27.00^{a}	0.000	45.67
% of TiC	4.426	2	2.213	69.99	27.00^{a}	0.000	30.51
Sliding velocity	1.7269	2	0.86343	27.31	27.00^{a}	0.001	11.63
Sliding distance	0.1619	2	0.08095	2.56	1.76^{d}	0.157	0.7
AXB	0.6090	4	0.15225	4.82	4.53^{b}	0.044	3.37
AXC	0.5157	4	0.12894	4.08	3.18^{c}	0.062	2.72
AXD	0.0762	4	0.01905	0.6	–	0.675	0.00
Residual error	0.1897	6	0.03162	–	–	–	5.40
Total	14.2994	26	–	–	–	–	100

*$a = 99.99\%$; $b = 95\%$; $c = 90\%$; $d = 75\%$.

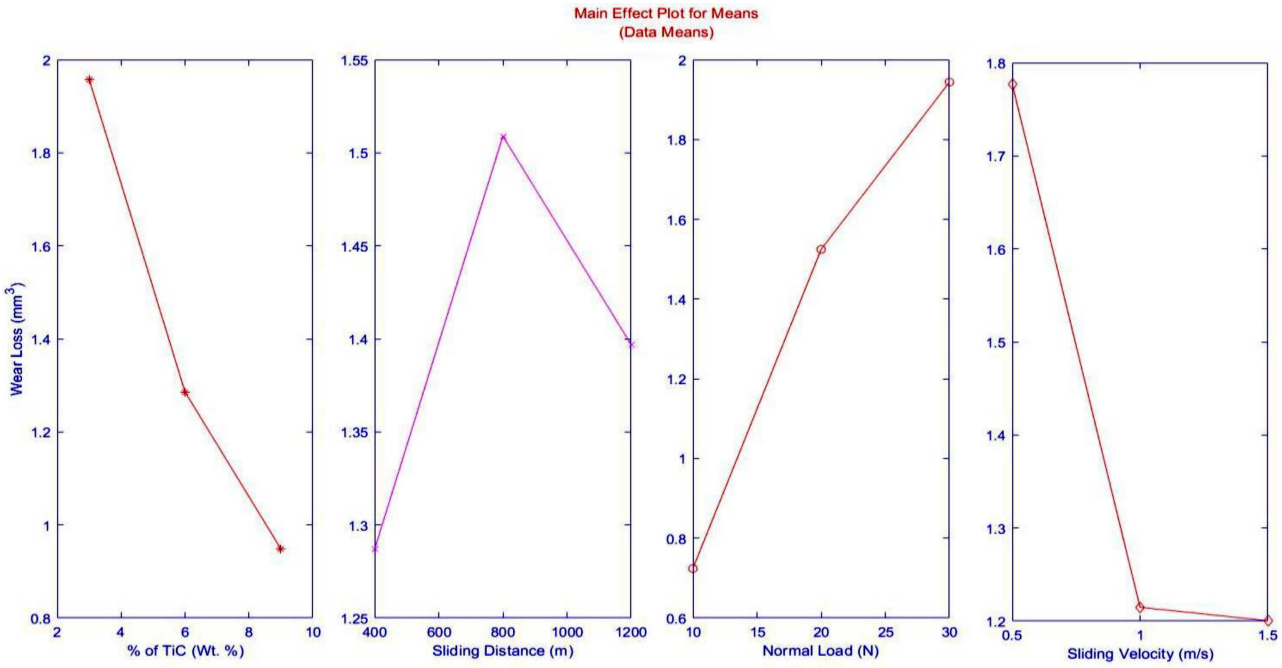

Figure 4. Main effect plot of studied parameters.

were highly significant contributing parameters within the studied range.

3.4.2. Effect of process parameters and their interaction

The main effect plots are shown in Figure 4. The advantage of main effect plots is it facilitates the evaluation of parameter influence on the response. In the current study main effect plot was used to analyze the effect of each parameter on wear loss of MMCs. Figure 5(a)–(f) illustrates the response surface contour plots suggesting the interaction of two individual parameters. The response surface and contour plots reveals the significance of interaction effect. However, approximately parallel lines on the contour plots were obtained (Figure 5(e)). It suggests that the load versus sliding velocity interaction effect was insignificant on wear. Also, based on the main effect plot of means of wear parameters, the determined optimized parameters levels to yield minimum wear loss for Al2025/TiC MMCs were 9%TiC reinforcement, 400 m sliding distance, 10 N normal load and 1200 m/s sliding speed.

The plots reveal that wear loss decreases drastically with the increase in % of TiC particle reinforcement and increases with the increase in load. The rise of sliding distance has increased the wear loss to a certain level and a further rise in sliding distance has caused reduction of wear loss. The increase of sliding speed resulted in the decrease of wear loss drastically till 2nd level, further decline of wear loss has occurred progressively with increase in speed.

3.5. Corelations with regression model

In addition to ANOVA analysis, regression analysis was employed to establish a correlation between wear

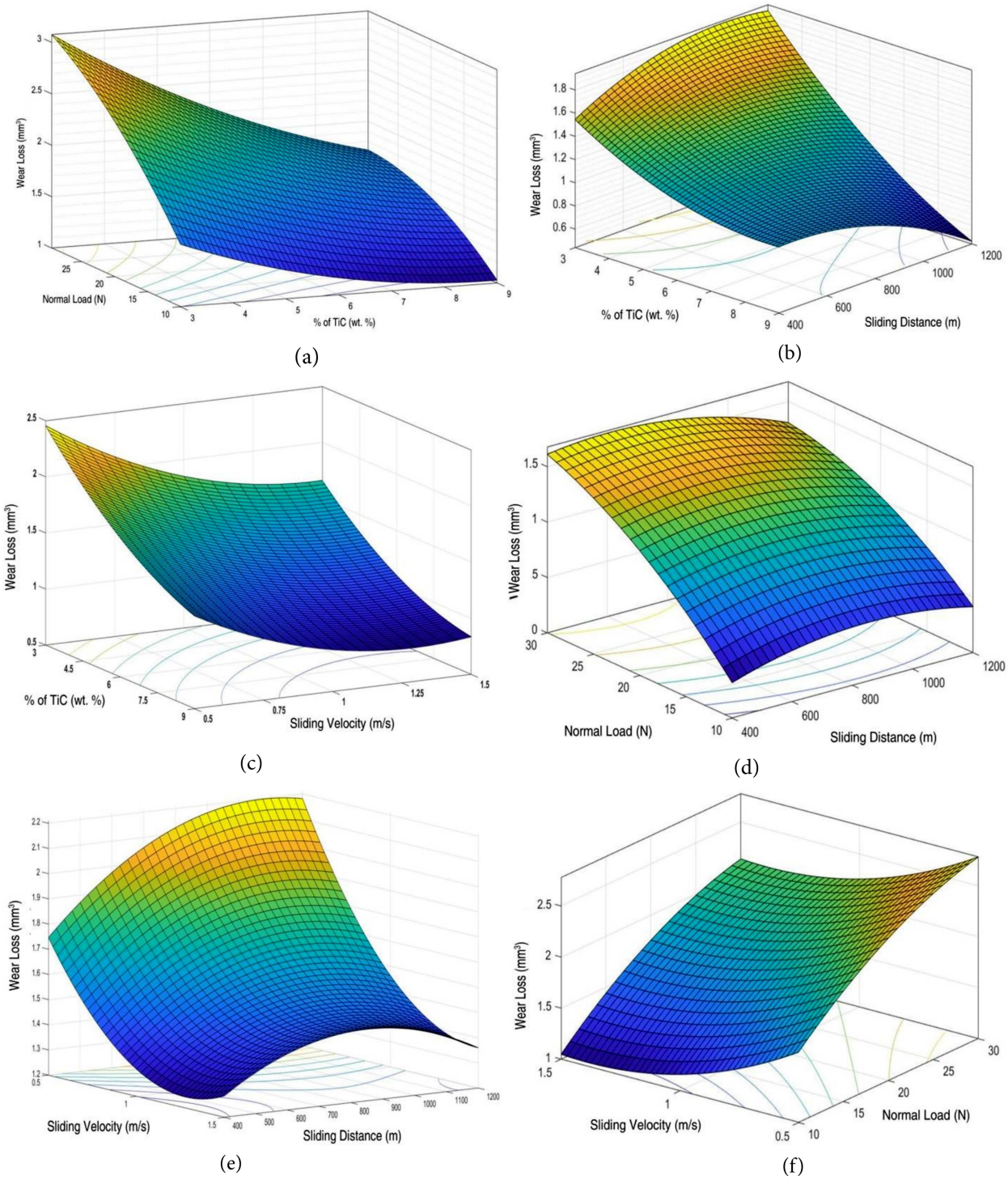

Figure 5. Response surface plot of studied parameters.

parameters and wear volume loss. The established regression model is presented as Eq. (11). The R^2, R^2 (Adj.) and R^2 (pred.) of the model were 99.29%, 98.58%, and 96.09%, which indicates that difference between R^2, R^2 (pred.) is less than 20% (0.2) and all values are higher 95%. Hence, it can be concluded that the presented model is adequate and feasible to predict the wear volume loss within the studied range of parameters.

$$Wear(\mathrm{mm}^3) = -0.122 - (0.1348 \times A) + (0.003530 \times B) + (0.1790 \times C) - (2.249 \times D)$$

$$+(0.01676\times A^2)-(0.000001\times B^2)$$
$$-(0.001619\times C^2)+(0.832\times D^2)$$
$$-(0.000185\times A\times B)-(0.006600\times A\times C)$$
$$+(0.0507\times A\times D)-(0.000025\times B\times C)$$
$$-(0.000451\times B\times D)$$

$$R^2-99.29\%;\ R^2\ (Adj.)-98.58;\ R^2\ (pred.)-96.09. \quad (11)$$

3.6. Wear analysis using SHO

SHO is a nature-inspired soft computing optimization technique. In the current investigation, wear loss optimized value was attained using a single-objective SHO optimization technique. The developed regression model (Eq. (11)) was utilized as a minimization function to SHO algorithm. The function was attempted to optimize within the objective space indicating the range of parameters considered in the work. The search agents and iterations were varied till better output was computed. The minimum wear loss value as optimal value was obtained with the corresponding wear parameters level combination. The optimal parameter levels combination is shown in Table 6 and compared with Taguchi optimized results. Also, further ensured with confirmation test conducted at optimal parameters level. The obtained results reveal that, SHO outperforms over the Taguchi optimization technique. Further, the deviation of predicted results with experimental results was relatively closer and within the acceptable range. The deviation was found less with optimized parameter level combination values of SHO technique. The convergence curve indicating a pattern of convergence of performance output with the number of iterations are illustrated in Figure 6. Hence, the SHO optimizer can be preferred over Taguchi's technique for the optimization of wear parameters. Also, prediction and optimization performance of wear parameters were found to be feasible and adequate. However, better efficiency concerned with the prediction of output can be enhanced with a large amount of experimental data.

3.7. Wear surface analysis

The dry sliding wear of MMCs phenomenon owes to the removal of surface asperities exists due to surface unevenness. Besides, it is aided with contact stress developed at the contact zone on interacting surface. Generally, relatively softer material pin being MMCs sample progressively loses its surface particles. The researchers are investigating to reduce it. In this regard, TiC as hard reinforcement particle is incorporated in MMCs.

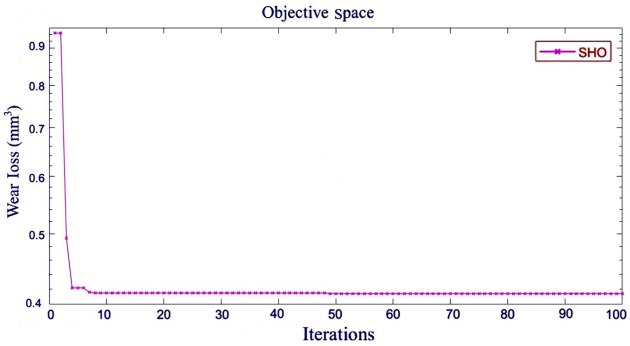

Figure 6. Convergence curve.

Further, at low load range, stress developed at the contact zone was relatively less causing low wear loss. The increase in normal load results in the increase of magnitude of contact stress developed, subsequently increases the friction between interacting surfaces. Thus, high temperature is generated resulting in softening of pin [27]. Besides, Al matrix alloy of MMCs is relatively more prone to softening at high temperatures compared to disc material. Hence, the pin surface has been easily detached at high load. Also, at high load conditions, cold welding occurs due to more significant temperature existence at the contact zone. Consequently, the transition of mild to severe wear phenomenon occurs.

The increase in the sliding distance has increased the wear loss from level 1 to level 2 of studied range. It is attributed to the fact that an increase in sliding distance increases the interaction of pin with counterface. It leads to the generation of heat energy due to prolonged higher friction. Also, it facilitates for the detachment of TiC particles from the matrix. The detached particle form a tribolayer acting as protective layer over pin and prevent direct contact of the pin with counterface. Thus, wear volume loss was reduced with a further increase in sliding distance. Similar results were reported by Sharma et al. [28] during dry sliding of Al/sillimanite MMCs. Furthermore, the increase

Table 6. Results of confirmation test for optimal level parameter combinations.

Technique	Optimized levels of parameters				Predicted result (mm^3)	Experimental result (mm^3)	Error (%)
	Normal load (N)	% of TiC (Wt. %)	Sliding velocity (m/s)	Sliding distance (m)			
Taguchi	10	9	1.5	400	0.4548	0.5046	9.87
SHO	10	9	1.5	981	0.1977	0.2038	3.46

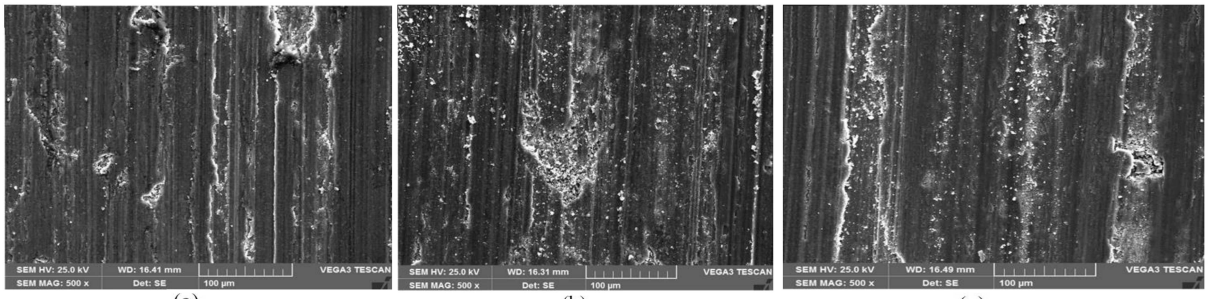

Figure 7. SEM image of worn surface of (a) Al2024+3%TiC, (b)Al2024+6%TiC, and (c)Al2024+9%TiC MMCs.

in sliding velocity increases the amount of tribolayer formation and hence decreases the kinematic friction at interaction zone of the contacting surface [29]. Therefore, decrease of wear volume loss with the increase in sliding velocity was noticed.

Figure 7(a), (b), and (c) indicates the salient features of worn surface morphology of Al2024 with 3%, 6%, and 9% TiC composites. The wear development occurring here concerned the ridge formation and material removal characterized by plastic deformation due to high load at 30 N. It also reveals discrete configuration of parallel furrows in the sliding direction. Besides, cracks are incremental to the subsurface of matrix, resulting in material loss in the form of debris. The wear loss due to plastic deformation is relatively more prominent in Al+3%TiC MMC (Figure 7(a)). Figure 7(b) and (c) illustrates the craters formed due to dislodgement of TiC particles from matrix. Also, the plastic deformation occurrence is less ascertained. It is attributed to the fact that hard reinforcement particle reinforcement causes a barrier for the penetration of asperities into pin surface. Thus, wear of pin material occurs only after either the detachment of TiC particle from matrix or deformation and shear of the particle due to high stress developed at the contact zone. Further, penetration of asperities requires energy greater the surface barrier energy grew due to the incorporation of TiC. The barrier energy increases with the increase in TiC reinforcement. Hence, MMCs with greater percentage of reinforcement can bear and resists the higher contact stress generated during sliding phenomenon. Therefore, increased TiC percentage reinforcement enhanced wear resistance of MMCs.

4. Conclusions

Based on the current study on mechanical and sliding wear behaviour or Al/TiC MMCs, following conclusions were drawn:

- In the current study, microstructure and mechanical charteristics of Al2024 matrix alloy reinforced with 3%, 6% and 9% TiCp MMCs were studied;
- Microstructural characterization illustrated uniform distribution of TiC in the Al2024 matrix with limited voids. The Al/9%TiC MMC exhibited better mechanical properties compared to other compositions;
- The optimization of wear parameters for minimum wear loss was achieved through novel metaheuristic Spotted Hyena Optimization (SHO) algorithm and compared with optimum value attained through Taguchi's method. The optimum values of both approaches were validated through experimental values;
- SHO approach has demonstrated better optimum value prediction with corresponding process parameters compared to Taguchi techique. Perhaps, SHO algorithm search for global optimum compared to local optimum value achieved through Taguchi method;
- The SHO (9.87% error) exhibited closeness between experimental and predicted values compared to Taguchi techniques (3.46% error). Thus, SHO approach is feasible in the selection of adequate wear parameters to achieve minimum wear of composites for engineering applications.

Funding

There is no funding for this research.

Conflicts of interest/Competing interests

There is no conflict of interest.

Availability of data and material

Not applicable.

Code availability

Not applicable.

Nomenclature

$\overrightarrow{D_h}$	Separation length of spotted hyena and prey
x	Means, present iteration
$\overrightarrow{B}, \overrightarrow{E}$	Vectors of coefficient
$\overrightarrow{P_p}, \overrightarrow{P}$	Location vectors of prey and spotted hyenas
$\|$ and $\times$	Absolute value and multiplication with vectors
$\overrightarrow{h}$	iterations
$r\overrightarrow{d_1}$ and $r\overrightarrow{d_2}$	Random vectors lie in interval of [0,1]
$\overrightarrow{P_h}$	Location of first feasible solution (hyena)
$\overrightarrow{P_k}$	Location of other spotted hyenas
N	Number of hyenas
$\overrightarrow{M}$	Vector randomly lies in the interval of [0.5,1]
$no.$	Number of solutions
$\overrightarrow{C_h}$	Set of N number of optimum solutions
C	Normal load
A	TiC %
D	Sliding velocity
B	Sliding distance

References

1. Siddesh Kumar, N.G., Suresh, R., and Shiva Shankar, G.S. "High temperature wear behavior of Al2219/n-B_4C/MoS_2 hybrid metal matrix composites", *Composite Communications*, **19**, pp. 61–73 (2020). https://doi.org/10.1016/j.coco.2020.02.011
2. Xu, G., Yu, Y., Zhang, Y., et al. "Effect of B4C particle size on the mechanical properties of B4C reinforced aluminum matrix layered composite", *Science and Engineering of Composite Materials*, **26**, pp. 53–61 (2018). https://doi.org/10.1515/secm-2018-0072
3. Ramadoss, N., Pazhanivel, K., Kumar, S.G., et al. "Effect of B_4C and SiC nanoparticle reinforcement on the wear behavior and surface structure of aluminum (Al6063-T6) matrix composite", *SN Applied Sciences*, **2**, 903 (2020). https://doi.org/10.1007/s42452-020-2712-5
4. Joshi, A.G., Manjaiah, M., Basavarajappa, S., et al. "Wear performance optimization of SiC-Gr reinforced Al hybrid metal matrix composites using integrated regression-antlion algorithm", *Silicon*, **13**, pp. 3941–3951 (2021). https://doi.org/10.1007/s12633-020-00704-x
5. Wahba, M., Kawahito, Y., Kondoh, K., et al. "A fundamental study of laser welding of hot extruded powder metallurgy (P/M) AZ31B magnesium alloy", *Materials Science and Engineering: A.*, **529**, pp. 143–150 (2011). https://doi.org/10.1016/j.msea.2011.09.010
6. Suresh, R. "Comparative study on dry sliding wear behavior of mono (Al2219/B4C) and hybrid (Al2219/B_4C/Gr) metal matrix composites using statistical technique", *Journal of the Mechanical Behavior of Materials*, **29**, pp. 57–68 (2020). https://doi.org/10.1515/jmbm-2020-0006
7. Reihanian, M., Asadullahpour, S.R., Hajarpour, S., et al. "Application of neural network and genetic algorithm to powder metallurgy of pure iron", *Materials and Design*, **32**, pp. 3183–3188 (2011). https://doi.org/10.1016/j.matdes.2011.02.049
8. Pandey, U., Purohit, R., Agarwal, P., et al. "Effect of TiC particles on the mechanical properties of aluminium alloy metal matrix composites (MMCs)", *Materials Today Proceedings*, **4**, pp. 5452–5460 (2017). https://doi.org/10.1016/j.matpr.2017.05.057
9. Gotagunaki, S., Mudakappanavar, V.S., and Suresh, R. "Investigation on microstructure and tensile fractography of RE Oxides (CeO2/Y2O3) reinforced AZ91D magnesium matrix composites", *Frattura ed Integritá Strutturale*, **63**, pp. 100–109 (2023). https://doi.org/10.3221/IGF-ESIS.63.10
10. Suresh, R., Joshi, A.G., and Siddeshkumar, N.G. "Investigation on dry sliding wear behavior of AA5083/nano Al_2O_3 metal matrix composites", *Revista de Metalurgia*, **58**, pp. 1–8 (2022). https://doi.org/10.3989/revmetalm.213
11. Riddhisha, C., Siddesh, B., Latha Shankar, B., et al. "Optimization and analysis of dry sliding wear behaviour of N-B4C/MOS2 unreinforced AA2219 nano hybrid composites using response surface methodology", *Metallurgical and Materials Engineering*, **28**, pp. 469–485 (2023). https://doi.org/10.30544/840
12. Mussatto, A., Ul-Ahad, I., Taherzadeh, R., et al. "Advanced production routes for metal matrix composites", *Engineering Reports*, **3**, pp. 1–25 (2021). https://doi.org/10.1002/eng2.12330
13. Ravikumar, M., Reddappa, H.N., Suresh, R., et al. "Optimization of wear behaviour of Al7075/SiC/Al_2O_3 MMCs using statistical method", *Advances in Materials and Processing Technologies*, **8**, pp. 4018–4035 (2022). https://doi.org/10.1080/2374068X.2022.2036583
14. Tarasasanka, C., Snehita, K., Ravindra, K., et al. "Optimization of dry sliding wear properties of AZ91E/nano-Al_2O_3 reinforced metal matrix composite with grey relational analysis", *International Journal of Engineering, Science and Technology*, **11**, pp. 41–48 (2019). https://doi.org/10.4314/ijest.v11i4.4
15. Natrayan, L. and Senthil Kumar, M. "Influence of silicon carbide on tribological behaviour of AA2024/Al_2O_3/SiC/Gr hybrid metal matrix squeeze cast composite using Taguchi technique", *Material Research Express*, **6**, 1265f9 (2019). http://dx.doi.org/10.1088/2053-1591/ab676d

16. Arunkumar, S., Ashokkumar, R., Sundaram, M.S., et al. "Optimization of wear behaviour of Al7075 hybrid metal matrix composites using Taguchi approach", *Materials Today: Proceedings*, **33**, pp. 570–577 (2020). https://doi.org/10.1016/j.matpr.2020.05.453

17. Miloradović, N., Vujanac, R., Stojanović, B., et al. "Dry sliding wear behaviour of ZA27/SiC/Gr hybrid composites with Taguchi Optimization", *Composite Structures*, **264**, 113658 (2021). https://doi.org/10.1016/j.compstruct.2021.113658

18. Velavan, K., Palanikumar, K., and Senthilkumar, N. "Experimental investigation of sliding wear behaviour of boron carbide and mica reinforced aluminium alloy hybrid metal matrix composites using Box-Behnken design", *Materials Today: Proceedings*, **44**, pp. 3803–3810 (2021). https://doi.org/10.1016/j.matpr.2020.12.333

19. Gangwar, S. and Pathak, V.K. "Dry sliding wear characteristics evaluation and prediction of vacuum casted Marble Dust (MD) reinforced ZA-27 alloy composites using hybrid improved bat algorithm and ANN", *Materials Today: Communications*, **25**, 101615 (2020). https://doi.org/10.1016/j.mtcomm.2020.101615

20. Gangwar, S., Sharma, S., and Pathak, V.K. "Preliminary evaluation and wear properties optimization of boron carbide and molybdenum disulphide reinforced copper metal matrix composite using adaptive neuro-fuzzy inference system", *Journal of Bio-Tribology and Corrosion*, **7**, 4 (2021). https://doi.org/10.1007/s40735-020-00444-w

21. Stalin, B., Kumar, P.R., Ravichandran, M., et al. "Optimization of wear parameters using Taguchi grey relational analysis and ANN-TLBO algorithm for silicon nitride filled AA6063 matrix composites", *Material Research Express*, **6**, 106590 (2019). http://dx.doi.org/10.1088/2053-1591/ab3d90

22. Aydin, F. "The investigation of the effect of particle size on wear performance of AA7075/Al_2O_3 composites using statistical analysis and different machine learning methods", *Advanced Powder Technology*, **32**, pp. 445–463 (2021). https://doi.org/10.1016/j.apt.2020.12.024

23. Dhiman, G. and Kumar, V. "Spotted hyena optimizer: A novel bio-inspired based metaheuristic technique for engineering applications", *Advances in Engineering Software*, **114**, pp. 48–70 (2017). https://doi.org/10.1016/j.advengsoft.2017.05.014

24. Panda, N., Majhi, S.K., and Pradhan, R. "A hybrid approach of spotted hyena optimization integrated with quadratic approximation for training wavelet neural network", *Arabian Journal of Science and Engineering*, **47**, pp. 10347–10363 (2022). https://doi.org/10.1007/s13369-022-06564-4

25. Ilany, A., Booms, A.S., and Holekamp, K.E. "Topological effects of network structure on long-term social network dynamics in a wild mammal", *Ecological Letters*, **18**, pp. 687–95 (2015). https://doi.org/10.1111/ele.12447

26. Sunar, T. and Özyürek, D. "Effect of Al_2O_3 Nanoparticles as reinforcement on the wear properties of A356/Al_2O_3 nanocomposites produced by powder metallurgy", *Journal of Tribology*, **144**, 081701 (2022). https://doi.org/10.1115/1.4053628

27. Khan, M.M., Dey, A., and Hajam, M.I. "Experimental investigation and optimization of dry sliding wear test parameters of aluminum based composites", *Silicon*, **14**, pp. 4009–4026 (2022). https://doi.org/10.1007/s12633-021-01158-5

28. Sharma, S., Nanda, T., and Pandey, O.P. "Effect of particle size on dry sliding wear behaviour of sillimanite reinforced aluminium matrix composites", *Ceramics International*, **44**, pp. 104–114 (2018). https://doi.org/10.1016/j.ceramint.2017.09.132

29. Lagisetti, V.K., Reddy, A.P., and Krishna, P.V. "Dry sliding wear study on AA6061/SiCp nano and AA6061/SiCp/Gr hybrid nanocomposites", *Silicon*, **14**, pp. 12235–12250 (2022). https://doi.org/10.1007/s12633-022-01908-z

Biographies

Rangappa Suresh is an Associate Professor in the Department of Mechanical and Manufacturing Engineering at MS Ramaiah University of Applied Sciences, Bangalore, India. He did his MSc (M Tech) and PhD in 2002 and 2013 from Kuvempu University, Karnataka, India. He has 24 years of experience in teaching research and industries. His areas of research interests include composites, surface coating, additive manufacturing, hard materials machining, numerical modelling, and experimental analysis of advanced materials.

Ajith G. Joshi presently serving as Assistant Professor in the Department of Mechanical Engineering, Madanapalle Institute of Technology and Science, India. He holds MSc from VTU, Belagavi and currently pursuing PhD in VTU, Belagavi. He has vast teaching experience of 14 years. His area of research interest includes tribology and machining of composite materials. He has published research articles in national and international journals, conference and edited book chapters.

Mallaiah Manjaiah is an Assistant Professor of Mechanical Engineering at NIT Warangal. He is holding degrees from University B.D.T College of Engineering, Karnataka (BE and M.Tech in Manufacturing), and National Institute of Technology Karnataka (PhD in Mechanical Engineering). He has vast experience in Welding and Additive Manufacturing, he has authored 40 journal articles, 12 book chapters, presented 15 papers worldwide, and conducted over 10 Additive Manufacturing training programs. Additionally, he has edited two books in welding and Additive Manufactur-

ing, published by Elsevier and Taylor and Francis.

Satish Kumar is an Assistant Professor in the Department of Mechanical Engineering and in charge of Advanced Manufacturing Technology Lab at Symbiosis Institute of Technology, Symbiosis International (Deemed University), Pune India. He completed his MSc (MTech-Tool Engineering) in 2013 and PhD in 2020 from K Visvesvaraya Technological University, Belgaum, Karnataka, India. He has over 8 years of experience in teaching, research, and industry. His areas of research interests include smart manufacturing, digital twin, condition monitoring, composites, cryogenic treatment, additive manufacturing, and Hard materials machining. He has authored more than 28 international/national journal and conferences publications.

Kurki Nagaraj Bharath is currently serving as Dean (Research and Innovation) and Professor in Department of Mechanical Engineering, GMIT, Davangere, INDIA. He has pursued his Post-Doc Research at Composite Material and Engineering Center, Washington State University, USA. His area of research includes Characterization of Natural fiber and its Composite materials, failure analysis and optimization. He has authored more than 55 publications in peer reviewed International Journals. Also, he has received research funds from government agencies. He has over 15 years of experience in teaching, research, and industry.